Corresponding Author Details:
A/Prof Mike Ford
Institute for Nanoscale Technology,
University of Technology, Sydney
PO Box 123
Broadway, NSW 2007
Australia

Tel: (61 2) 9514 7956 Fax: (61 2) 9514 7553
Email: mike.ford@uts.edu.au

The effect of surface symmetry on the adsorption energetics of SCH_3 on gold surfaces studied using Density Functional Theory

C. Masens, M.J. Ford* and M.B. Cortie

Institute for Nanoscale Technology,

University of Technology Sydney, PO Box 123, Broadway, NSW 2007, Australia

Adsorption of methanethiol onto the three, high symmetry gold surfaces has been studied at the density functional level using a linear combination of atomic orbitals approach. In all three cases the bond energy between the thiolate radical and surface is typical of a covalent bond, and is of the order of 40 kcal.mol^{-1}. For the (111) the fcc hollow site is slightly more stable than the bridge site. For the (100) surfaces the four-fold hollow is clearly the most stable, and for the reconstructed (110) surface the bridge/edge sites either side of the first layer atoms are preferred. The calculated differences in binding energy between the three surfaces indicate that the thiolate will preferentially bind to the Au(110) or (100) before (111) surface, by about 10 kcal.mol^{-1}. The (110) surface is slightly more favourable than the (100), although the energy difference is only 3 kcal.mol^{-1}. The results suggest the possibility of selectively functionalising the different facets offered by a gold nanoparticle.

* Corresponding author email: mike.ford@uts.edu.au

Keywords: Density functional calculations; Surface chemical reaction; gold, carbon, sulphur, hydrogen; thiol; adatoms;

INTRODUCTION

Since the early 1980's there has been an increasing interest in self-assembled monolayers (SAMs) [1] as a means of controlling the surface properties of noble metals, and in particular gold [2,3]. These systems also provide a convenient platform for attaching a wide range of functional groups (including biomolecules) to the surface with potential applications in molecular electronics and sensors [4,5].

The most commonly studied systems are thiolates, and in particular alkanethiols, adsorbed onto the Au(111) surface [6,7]. The Au(111) surface is chemically inert and it is easy to prepare surfaces relatively free of contaminant molecules. The Au-S bond is energetically quite stable and so high quality, ordered monolayers are also relatively easy to prepare. Thiolate ligands adsorbed onto Au(111) are therefore model systems for investigating how surface properties such as wetting [8,9], friction [4,10], and conduction [11] can be tuned via SAMs. A variety of experimental techniques have been employed to characterise the structure and properties SAMs including ellipsometry [9,12], atomic force microscopy [7,13], scanning tunneling microscopy [14], x-ray diffraction [15], contact angle [9,12], and Fourier transform infra-red spectroscopy [16].

Theoretical studies also play an important role in understanding the properties and behaviour of SAMs. Molecular mechanics methods can simulate the dynamic behaviour of a SAM consisting of many thousands of molecules, but depend upon an *a priori* knowledge of the various interactions. First principles and semi-empirical studies can map the potential energy surface of the gold-thiolate molecular interaction and identify preferred adsorption geometries and binding energies. The literature contains a number of such studies [17] [18-21], but has generally followed the experimental lead and been confined to the Au(111) surface.

In the present study we are interested in exploring these issues, and more importantly extending our knowledge to the other high symmetry surfaces, namely the (110) and (100) surfaces. This has important implications not only to our understanding of the energetics of the bulk surfaces but to the structure of gold nanoparticles. These are finding increasing application as building blocks in a variety of nanostructures and devices due to their unusual chemical reactivity and optical properties such as infrared adsorption [22]. They are commonly prepared through wet chemical means and are thus usually surface passivated. In addition, by investigating the relative adsorption energetics of these surfaces it may be possible to devise strategies for controlling the growth of nanoparticles or preferentially functionalising the different surfaces presented by the nanoparticle.

Below we present the results of a Density Functional theory study of adsorption of the SCH_3 molecule onto the Au(111), (110) and (100) surfaces. For each surface we have identified the preferred binding site and binding energy. In all our calculations full coverage is used, that is all the equivalent adsorption sties are occupied by an adsorbate molecule. Although this is a rather simplified system compared to experimental SAMs which use more complex molecules, it is nonetheless the appropriate starting point for these studying larger systems and provides important parameters for empirical calculations of more complex systems.

CALCULATION METHODS

Our calculations were performed using the SIESTA [23] code. This package implements Density Functional Theory (DFT) [24] within the linear combination of atomic orbitals (LCAO) approximation. The generalised gradient approximation (GGA) was employed using the PBE exchange-correlation functional [25]. All calculations were spin unrestricted.

Core pseudopotentials for Au, S, C, and H were constructed according to the scheme developed by Troullier and Martins [26], with relativistic corrections used in the case of Au atoms. Cut-off radii for Au were 2.35 a.u. for l = 0,1, and 1.5 a.u. for l = 2 and 3. Cut-off radii for C, S and H were 1.34, 1.5 and 1.25 a.u. respectively, independent of l. The 1s electron of H, 2s and 2p of C, 3s and 3p of S, and the 6s and 5d of Au are described by a double-zeta basis set with a polarization function. The atomic orbitals are strictly localised in SIESTA, falling to zero outside a cut-off radius. The cut-off radius is specified by giving an energy-shift, that is the energy rise in the orbital due to confinement, and a compromise is sought between computational speed and cut-off. Figure 1 shows the total energy of the SCH_3 molecule and gold slab as a function of energy-shift. Adsorption energies were calculated using an energy shift of 0.0005 Ry, where total energies are converged to about 0.05 eV. The equivalent plane-wave cut-off of our calculations is 110 Ry.

Geometry optimisations were performed using the conjugate gradient method with a convergence criteria of 0.04 eV.Å^{-1}. The default convergence criteria for the SCF cycles at each stage of structure optimisation was used, that is 10^{-4} eV.

The well known basis set superposition error (BSSE) is inherent to atomic orbital based self-consistent calculations, and will introduce an error into the calculated interaction energies, in this case adsorption energies. Imbalance in the basis sets used to describe the interacting particles lead to variational differences and commonly results in overestimates of the interaction [27]. Counterpoise corrections as described by Boys and Bernardi [28] have been used in this work to attempt to estimate this error in our adsorption energies. The total system energy for adsorbate-substrate was first calculated then the energies for the separated substrate and adsorbate by ghosting the appropriate set of atoms was calculated. In this way the total system, and its separated constituents have exactly the same variational degrees of freedom. The corrections behave as expected making the energies of the separated

components more negative and reducing the binding energy compared with having no BSSE corrections. For the three surfaces studied, adsorption energies are reduced by about 10 % after counterpoise correction.

The SIESTA code employs periodic boundary conditions. Calculations for the gas phase thiol molecule were carried out by placing the molecule in a sufficiently large unit cell so that interaction between the periodically repeated molecules was negligible. A lattice parameter of 10 Å was used. Only a single k-point is required for the molecular calculation. In the case of bulk gold or gold slabs a 7x7x7 (196 k-points) or 7x7x1 (28 k-points) Monkhorst-Pack [29] k-grid was found to give a reasonably converged total energy. Figure 2 shows the energy of the bulk gold unit cell as a function of the number of k-points. The variation in energy beyond 196 k-points is only about 0.01 eV. A 7x7x7 k-grid is therefore sufficient for bulk calculations, and a 7x7x1 k-grid for the slab calculations.

As a preliminary test of the calculations a geometry optimisation of the gas phase molecule was performed giving a geometry in good agreement with experiment. As a further test of the quality of the pseudopotentials employed we have also calculated the bulk lattice parameter for Au at the local density approximation (LDA) (using the Ceperley-Adler functional [30]) and GGA (PBE functional [25]) level. The LDA calculation gives a lattice parameter of 4.097 Å compared with the experimental value of 4.0782 Å [31]. Inclusion of gradient corrections expands the lattice parameter to 4.187 Å.

Adsorption calculations were performed with a 5 layer slab and a 10 Å vacuum gap in the *z* direction. With metallic substrates relatively thick slabs are required in order to reproduce adequately a bulk material terminated by a single surface. Five layers is about as thick as practicable in terms of computational resources, and gives adsorption energies that are converged to about 2 kcal.mol^{-1}[19-21,32,33].

Our methodology for investigating the adsorption energetics has been to find the global minimum of adsorbate plus substrate for the three surfaces. Rather than perform complete relaxation of five layer slab + molecule (which is a prohibitively large calculation) we initially optimise the slab and molecule independently. The relaxed molecule is then placed 2 Å above the relaxed slab at various initial sites, and the adsorbate and surface layer of the slab undergoes a further unconstrained relaxation. From the symmetry of the (111), (110) and (100) surfaces only a limited number of starting points for the adsorption calculations were needed for each surface, these are shown in the lower part of Figure 3. The upper part of this figure shows how these surfaces relate to the facets of a gold nanoparticle. This is in contrast to other work in the literature where it is common to move a rigid molecule across the surface and map out the potential energy surface. Both have their advantages and disadvantages. Our method should, in principle, find the optimum adsorption geometry and energy.

The unit cell of the five layer slab has been chosen such that for the adsorption calculations there is full coverage, that is for any one calculation all symmetry equivalent sites will be occupied by a thiol molecule. It must be remembered, however, that the (110) surface undergoes a (2x1) reconstruction, as discussed below, so that the absolute coverage in this case is lower than the other two surfaces. The unit cell used for the (110) surface is effectively twice as big as the (111) or (100) surfaces. A 2x2 surface unit cell for the (111) and (100) adsorption calculations was used, giving a separation of nearly 6 A between adjacent adsorbed sulphur atoms. Spacing between molecules on the (110) surface is even larger. It is expected that interaction between adjacent molecules is negligible.

RESULTS AND DISCUSSION

A. Relaxation of the Au Substrates

Five layer gold slabs, for each of the surface symmetries (111), (110) and (100) were relaxed by geometry optimisation keeping only the deepest layer atoms constrained in their positions. The results are shown in Table 1. We have presented the relaxation of the layer spacings in terms of the average *z* positions of the atoms in each layer.

For the (111) surface, the overall behaviour of the slab is a contraction, which is consistent with expectation, since the surface possesses none of the symmetries in *z* that exist in the bulk. The spacing changes in percentage terms were found to be (counting the surface layer as the ~~zeroth~~ 1st layer) d_{12} equal to –1.43 %, d_{23} equal to –2.35 %, d_{34} equal to –2.25 %, d_{45} equal to –0.48 %. Since only the bottom layer of atoms is constrained in our calculation the slab has two surfaces and both surfaces are allowed to relax. At first it seems surprising that the relaxations are therefore not symmetric with respect to the two surfaces, that is the contraction in d_{12} would equal d_{45}, and d_{23} would equal d_{34}. The results indicate that while the change in d_{23} does indeed equal d_{34}, the changes in d_{12} and d_{45} are not equal. One explanation for this is that the packing sequence of layers repeats every 4th layer (due to the ABC packing sequence of the FCC lattice). Hence the first and fifth layers of our slab are not in fact identical.

Our calculations give the relaxed (110) surface as the so-called missing row (1x2) reconstruction as reported by Hofner and Rabelias [34] and others. The structure of the (1x2) reconstruction has been studied in detail by a number of experimental means. The consensus is in favour of the missing row model (MRM) in which every second $[1\bar{1}0]$ row is missing, and the accepted picture involves contraction of the outer layer, small pairing of the next layer, and buckling of the third layer. Compared to the other surfaces under consideration here, ~~T~~the Au(110)~~his~~ surface relaxation shows a much greater change of interlayer spacings, with d_{12} equal to –24.16 %, d_{23} equal to –21.17 %, d_{34} equal to –8.31 % and d_{45} equal to –20.00 %. In order to check whether the thickness of the slab effects the surface

relaxation in this case we repeated the calculation for a 10-layer slab. The results are entirely consistent with those reported in Table 1. In addition, a 10 layer slab without the missing row surface reconstruction also shows a substantial decrease in interlayer spacing. The large relaxation is a property of the open (110) surface and is not necessarily attributable to the missing row. In this case because the fifth layer atoms are fixed they cannot reconstruct to form the missing row pattern, hence we expect an asymmetry in the layer spacings of opposite faces of the slab. The value we~~s~~ obtained for the contraction of the first layer d_{12}~~$_{01}$~~ (~ -0.3 Å) ~~are~~ is consistent with those reported (both theoretical and experimental) elsewhere in the literature [35], which range from -0.16 Å to -0.40 Å. However, there is a disagreement with the d_{23} spacing change which is reported to be in the range – 0.04 Å to – 0.07 Å, while we found a value of –0.31 Å. The pattern that emerges in our results shows a similar degree of contraction in d_{12}, d_{23} and d_{45}, with d_{34} being around one third the size of the other spacing changes. This is unlike the findings of other groups, where there is a larger change in the outer spacing d_{12}, followed by much less pronounced changes in the next two deeper spacings.

Formatted

Formatted

Formatted

Formatted

Formatted

Formatted

For the (100) surface the spacing changes in percentage terms were found to be (counting the surface layer as the ~~zeroth~~ 1st layer) d_{0}~~$_{1}$~~$_{2}$ equal to –1.38 %, d_{1}~~$_{2}$~~$_{3}$ equal to –0.50 %, d_{2}~~$_{3}$~~$_{4}$ equal to –0.73 %, d_{3}~~$_{4}$~~$_{5}$~~$_{4}$ equal to –1.22 %. In this case there is a symmetry between the relaxation of the two sides of the slab because the repeat sequence is every other layer, hence the first and fifth layer are now identical.

B. Adsorption

Before describing the results of adsorption calculations for the three surfaces it is important to emphasise that the adsorbate is not constrained to remain at the initial site during relaxation. However, provided there is a minimum close to the starting point then the

adsorbate will not substantially alter its position. The starting points of the optimisations have been chosen to reflect the most likely, stable adsorption sites for each surface based upon consideration of the surface symmetry. In the light of this approach it is convenient to refer to each case by its identifying letter, rather than to use the usual surface site designation. This convention will be maintained throughout the remainder of this paper. Neither are the surface layer of gold atoms restrained to stay in their initial positions from the slab relaxations. In practice, it turns out that further relaxation of the surface driven by the presence of the adsorbate is small, with gold atoms closest to the molecule moving by less than 5 % of the layer spacing.

Four sites were used as starting points for full geometry optimisations, as shown in the leftmost image of Figure 3. The final adsorption energies, tilt angle of the adsorbate with respect to the surface normal, and distances to the nearest surface gold atoms are given in Table 2. In the *a*, *b* and *c* cases there are two nearest neighbour surface Au atoms to which the sulphur atom bonds, whereas in case *d* there are 3 equidistant surface atoms. The corresponding final adsorption geometries are shown in Figure 4. The starting configurations *b* and *c* give the most stable optimised geometries. The adsorption energies, tilt angle and adsorption height are the same for these two starting points, within the reliability of the calculation. However, as can be seen from Figure 4 the final adsorption site is different (*b* corresponds to the sulphur atom sitting above the fcc hollow site and *c* to the bridge site). In these two cases the starting point for the optimisation was indeed close to the final point, that is the fcc site for *b* and bridge site for *c*

A Mulliken population analysis indicates there are significant concentrations of charge between the S atom and two Au atoms in each case for both the *b* and *c* configurations. In the *b* case, there is 0.21*e* of charge recorded as the overlap population between the S atom and the two bonded Au atoms, as compared to 0.08*e* and 0.008*e* to the

other surface Au atoms. The overlap population between the S and C in this case is 0.82*e*. In the *c* case, there is 0.21*e* of charge recorded as the overlap population between the S atom and the two bonded Au atoms, as compared to 0.08*e* and 0.038*e* to the other surface Au atoms. The overlap population between the S and C in the *c* case is 0.83*e*. This is in contrast to the electron distribution calculated in ref [19], where a relatively uniform electronic charge density was found to exist between the S and each of the three nearest Au atoms. The primary contribution to the Au-S bond is the hybridisation between the S 3p orbitals and the Au 5d orbitals.

The *a* and *d* starting sites correspond to the on-top and hcp hollow respectively. From Figure 4 it is clear that after optimisation the sulphur headgroup ends up in the same hcp hollow site for both these starting positions. The final geometry of the thiol molecule is different in the two cases with the S-C bond tilting 53 and 37 degrees away from the surface normal respectively. This would suggest that there may be a number of local minima in the potential energy surface at this adsorption site with respect to tilting of the methyl group around the sulphur atom. Hence the adsorption energies are also slightly different. In all cases except *d*, the interatomic Au-S distances range between 2.50Å and 2.54Å, while the *d* case results were between 2.61Å and 2.62Å. Mulliken population analysis in the *d* case shows the Au-S overlap populations between the S and the three surrounding Au Atoms to be 0.15*e*, 0.16*e* and 0.19*e*, (*e* being the unit of electron charge).

From the above results there are three adsorption sites on the Au(111) surface: the fcc hollow, bridge and hcp hollow site. The hcp and bridge sites are the more energetically stable, both with adsorption energies of approximately 39 kcal.mol^{-1}. In both cases the tail of the adsorbed thiol tilts at an angle of 42 degrees from the surface normal, compared with the experimental value of 28-30°[3]. The hcp hollow site is less stable by about 6 kcal.mol^{-1}. The on-top site is not a local minimum for adsorption. This last point is clearly illustrated in

Figure 5 where the total energy of adsorbate plus substrate is plotted as a function of the sulphur-substrate distance for each of the four starting points. In this case the shape and orientation of the molecule relative to the surface is held fixed and only the height of the molecule above the surface varied. Minima occur for the fcc, hcp and bridge sites with the optimum height occurring at around 2.05Å in each case. By contrast the on-top site is unbound.

Comparing our results for Au(111) with previous work summarised in table 3 we find that there is good agreement between our results and those of Yourdshahyan *et al* [20]. There are differences of opinion over the location of the predicted preferred sulphur binding sites for thiols (usually SCH_3) on the Au(111) surface. Yourdshahyan et al [20] and (separately) Andreoni et al [19] have reported that the preferential binding site for SCH_3 was the fcc site, in contrast to the findings of Beardmore [18,36] and co-workers and also Sellers et al [37], who calculated that the hcp site was preferred. Hayashi *et al* [38] reported in 2001 that the bridge site (slightly off centred towards the fcc hollow site) was the preferred site for methyl thiolate. Vargas *et al* found in favour of the fcc site [33]. In 2002 Molina and Hammer [21] reported finding that the bridge site was energetically favoured. Fischer et al reported in 2003 [39] that bridge site was favoured for $C_{10}H_{21}S$, in contrast to the group's earlier published work for SCH_3 [19]. Majumder et al [40] in 2003 found the threefold coordination site on a truncated model of an Au(111) surface. Direct comparison of these results is difficult due to differences of approaches, because some groups are examining clusters while others are using slab geometries in periodic systems, and further, not all slabs have the same number of layers. A further difficulty lies in the different computational approaches taken by various groups, with some using plane wave codes [20,21] while others[18,36] have used LCAO based codes.

The reconstructed (110) surface of gold was sampled at eight starting locations as specified in Figure 3 above. The results of the geometry optimisation from these 8 starting points are given in Table 4 with the final geometries shown in Figure 6. There are two minima with respect to the location of the sulphur head group over the substrate. Starting points *a, b, c, e, f* and *g* all relax to the thiol adsorbed over the step edge formed by the missing row of gold atoms. The orientation of the methyl group with respect to the substrate following relaxation varies amongst the 6 starting points giving adsorption energies that are either close to 47 kcal.mol^{-1} or 51 kcal.mol^{-1}. Clearly there are, again, a number of local minima with respect to rotation of the methyl group around the sulphur atom. This is an important point and demonstrates that attempting to locate adsorption sites by potential energy surface mapping with rigid molecule in a fixed orientation is problematic. Staring points *d* and *h* relax to the same adsorption site where the sulphur is located above the hollow. Two different adsorption energies, 41 and 36 kcal.mol^{-1} are found in this case due, again to the orientation of the methyl group, however both are significantly lower than the step edge site.

There are two adsorption sites on the reconstructed (110) surface. Adsorption at the step edge formed by the missing row is the more energetically stable with an adsorption energy of approximately 51 kcal.mol^{-1}. The four-fold hollow adsorption site has an adsorption energy of approximately 41 kcal.mol^{-1}. It appears that the preferred tilt angle for the methyl group relative to the surface normal for both adsorption sites is of the order of 35 degrees.

The Mulliken overlap population analysis shows a similarity of bond formation in the *a, b, c, e, f* and *g* cases with an average Au-S bond population of 0.16*e*, whereas there are distinct differences with the *d* and *h* cases, with the d case Au-S population overlaps are an average of 0.4*e* lower in charge than the other cases, which is consistent with the weaker

adsorption energy in that instance. The *h* case is dissimilar from all other cases in the Au-S overlap populations, with bond populations of 0.19*e*, 0.11*e* and 0.11*e*, the only result that indicates, for this surface, that three Au atoms are involved

Only three starting sites were necessary for the Au(100) surface, given its high degree of symmetry. These are shown in Figure 3. Results of the relaxation from these three sites are given in Table 5 and shown in Figure 7. These three starting geometries all relax to the same final adsorption site with the sulphur atom sitting in the four-fold hollow. The adsorption energies range over approximately 5 kcal.mol^{-1} depending upon the final orientation of the methyl group. The maximum adsorption energy occurs with the methyl tilted at 49 degrees to the surface normal and gives an adsorption energy of 48 kcal.mol^{-1}.

Mulliken population analysis reveals the Au-S overlap populations in the *a* case to be significant (greater than 0.1*e*) with respect to only one of the nearby gold atoms, and in the *c* case there are no charge concentrations above 0.1*e* between the S and any of the neighbouring Au atoms. In the *b* case, the Au-S overlap populations are 0.17*e* with the two nearest neighbour gold atoms, in a geometry similar to that seen on the Au(111) surface (cases *b* and *c*).

CONCLUSIONS

In this paper we have reported *ab initio* calculations of the adsorption of methane thiol on the three high symmetry gold surfaces. A density functional method within the linear combination of atomic orbitals approximation has been used to perform unconstrained relaxation of the molecular adsorbate on a previously relaxed 5 layer substrate. Starting geometries for the relaxations have been chosen based upon the symmetry of each surface, with 4, 8 and 3 starting geometries for the (111), (110) and (100) surfaces respectively. Double-zeta basis sets with a single polarisation function were used throughout to represent

the valence electrons, with the core electrons replaced by pseudopotentials. This representation reproduces the experimental gas phase structure of methane thiol and crystal structure of bulk gold well.

Relaxation of the five layered substrates produces a contraction of the surface layers of the order of a few percent for (111) and (100) surfaces. The calculations give a reconstruction of the (110) gold surface to produce the well-known missing row structure. This surface reconstruction is accompanied by a strong contraction of the surface interlayer spacing of the order of 20 %.

The most energetically stable adsorption sites for the three relaxed surfaces have been identified, these are the fcc hollow, step-edge and four-fold hollow for (111), (110) and (100) surfaces respectively. The (110) surface is the most open and reactive of the three and as expected gives the largest adsorption energy: 51 kcal.mol^{-1}. The (100) and (111) are less so with adsorption energies of 48 kcal.mol^{-1} and 39 kcal.mol^{-1} respectively. However, whether the present calculations are capable of resolving unambiguously energy differences of 3 kcal.mol^{-1} is debateable. The single largest source of error is likely to be the basis set superposition error. We have attempted to account for this using counterpoise corrections, albeit only as an estimate of this error.

The present work is a first attempt at answering the question of whether it is possible to selectively functionalise the three high symmetry surfaces of gold. It deals with a rather idealised system involving gas-phase adsorption of isolated molecules, but is the appropriate staring point. The results of the calculations indicate that it is indeed possible to selectively adsorb to the (110) or (100) surface compared with the (111) surface, the energy difference being 10 kcal.mol^{-1}. Evidence for selective adsorption between the (110) and (100) surfaces is less definite from our calculations with the energy difference of 3 kcal.mol^{-1} falling close to the likely reliability of the calculations. The interaction between the tail groups when the

adsorbates are close-packed into a self-assembled monolayer, which is mainly dispersive in nature, is not captured in the above DFT calculations. One might anticipate that the adsorption is dominated by the sulphur-gold interactions, while interactions between the adsorbed molecules determine the details of the molecular orientation within the SAM.

ACKNOWLEDGEMENTS

This work was supported by the University of Technology, Sydney. Computing resources were accessed through the merit allocation schemes of the APAC National facility and AC3 in NSW. The authors are indebted to Richard Leow at AC3 for technical support.

REFERENCES

[1] D. L. Allara and R. G. Nuzzo Journal Of The American Chemical Society 105 (1983) 4481; D. L. Allara and R. G. Nuzzo Langmuir 1 (1985) 45.

[2] A. Ulman, An Introduction to Organic Thin Films from Langmuir-Blodgett to Self Assembly, 1 ed. Academic Press Inc., San Diego, (1991).

[3] A. Ulman Chemical Reviews 96 (1996) 1533.

[4] C. Frisbie, L. Rozsnyai, A. Noy, M. Wrighton, and C. Lieber Science 265 (1994) 2071.

[5] A. Noy, D. Vezenov, and C. Lieber Annual Review of Materials Science 27 (1997) 381.

[6] G. E. Poirier Langmuir 13 (1997) 2019; G. E. Poirier and E. D. Pylant Science 272 (1996) 1145; P. Fenter, A. Eberhardt, and P. Eisenberger Science 266 (1994); D. A. Hutt and G. J. Leggett Langmuir 13 (1997) 3055; K. Tamada, J. Nagasawa, F. Nakanishi, K. Abe, T. Ishida, M. Hara, and W. Knoll Langmuir 14 (1998) 3264.

[7] G. Nelles, H. Schonherr, G. J. Vancso, and H. J. Butt Applied Physics a 66 (1998) S1261.

[8] P. E. Laibinis, C. D. Bain, R. G. Nuzzo, and G. M. Whitesides Journal of Physical Chemistry 99 (1995) 7663; S. V. Atre, B. Liedberg, and D. L. Allara Langmuir 11 (1995) 3882; P. A. DiMilla, J. P. Folkers, and H. A. Biebuyck Journal of the American Chemical Society 116 (1994) 2225.

[9] A. N. Parikh, D. L. Allara, I. B. Azouz, and F. Rondelez Journal of Physical Chemistry 98 (1994) 7577.

[10] A. Noy, C. D. Frisbie, L. F. Rozsnyai, M. S. Wroughton, and C. M. Leiber Journal of the American Chemical Society 117 (1998) 7943; M. K. Chaudhury Current Opinion in Colloid & Interface Science 2 (1997) 65; H. I. Kim, T. Koini, T. R. Lee, and S. S. Perry Langmuir 13 (1997) 7192.

[11] W. Mizutani, T. Ishida, and H. Tokumoto Japanese Journal of Applied Physics Part 38 (1999) 3892; T. Ishida, W. Mizutani, N. Choi, U. Akiba, M. Fujihira, and H. Tokumoto Journal of Physical Chemistry B 104 (2000) 11680; W. H. Han, E. N. Durantini, T. A. Moore, A. L. Moore, D. Gust, P. Rez, G. Leatherman, G. R. Seely, N. J. Tao, and S. M. Lindsay Journal of Physical Chemistry B 101 (1997) 10719.

[12] H. A. Biebuyck, C. D. Bain, and G. M. Whitesides Langmuir 10 (1994) 1825.

[13] A. Noy, C. Sanders, D. Vezenov, S. Wong, and C. Lieber Langmuir 14 (1998) 1508; K. Sasaki, Y. Koike, H. Azehara, H. Hokari, and M. Fujihira Applied Physics a 66 (1998) S1275; T. Uchihashi, T. Ishida, M. Komiyama, M. Ashino, Y. Sugawara, W. Mizutani, K. Yokoyama, S. Morita, H. Tokumoto, and M. Ishikawa Applied Surface Science 157 (2000) 244.

[14] R. K. Smith, S. M. Reed, P. A. Lewis, J. D. Monnell, R. S. Clegg, K. F. Kelly, L. A. Bumm, J. E. Hutchison, and P. S. Weiss Journal of Physical Chemistry B 105 (2001) 1119; C. B. Gorman, Y. F. He, and R. L. Carroll Langmuir 17 (2001) 5324; G. E. Poirier and M. J. Tarlov Langmuir 10 (1994) 2853.

[15] G. Y. Liu, P. Fenter, C. E. D. Chidsey, D. F. Ogletree, P. Eisenberger, and M. Salmeron Journal of Chemical Physics 101 (1994) 4301; M. Murphy, C. Nordgren, and R. Fischetti Journal of Physical Chemistry 99 (1995) 14039; J. J. Gerdy and W. A. Goodard Journal of the American Chemical Society 118 (1996) 3233; B. Gregory, R. Dluhy, and L. Bottomley Journal of Physical Chemistry 98 (1994) 1010.

[16] K. Tamada, J. Nagasawa, F. Nakanishi, K. Abe, M. Hara, W. Knoll, T. Ishida, H. Fukushima, S. Miyashita, T. Usui, T. Koini, and T. R. Lee Thin Solid Films 329 (1998) 150; W. Li, V. Lynch, and T. Heike Journal of the American Chemical Society 119 (1997) 7211.

[17] J. J. Gerdy and I. Willam A. Goodard J. Am. Chem. Soc. 118 (1996) 3233; W. Mar and M. L. Klein Langmuir 10 (1994) 188; M. Grunze and A. Pertsin Journal of Molecular Catalysis A-Chemical 119 (1997) 113; T. Bonner and A. Baratoff Surface Science 377 (1997) 1082.

[18] K. M. Beardmore, J. D. Kress, N. Gronbechjensen, and A. R. Bishop Chemical Physics Letters 286 (1998) 40.

[19] W. Andreoni, A. Curioni, and H. Gronbeck International Journal of Quantum Chemistry 80 (2000) 598.

[20] Y. Yourdshahyan, H. K. Zhang, and A. M. Rappe PHYSICAL REVIEW B, 63 (2001) 081405; Y. Yourdshahyan and A. M. Rappe J. Chem. Phys. 117 (2002) 825.

[21] L. M. Molina and B. Hammer Chem. Phys. Lett. 360 (2002) 264.

[22] P. D. O'Neal, L. R. Hirsch, N. J. Halas, J. D. Payne, and J. W. West Cancer Letters (2004).

[23] P. Ordejon, E. Artacho, J. M. Soler, Phys. Rev. B (Rapid Comm.) 53 (1996) R10441; J. M. Soler, E. Artacho, J. Gale, A. Garcia, J. Junquera, P. Ordejon, D. Sanchez-Portal J. Phys.: Condens. Matter, 14 (2002) 2745.

[24] W. Kohn and L. J. Sham Physical Reviews 140 (1965) A1133.

[25] J. P. Perdew, K. Burke, and M. Ernzerhof Phys. Rev. Lett. 77 (1996) 3865.

[26] N. Troullier and J. L. Martins Physical Review B 43 (1991) 1993.

[27] P. Valiron and I. Mayer Chem. Phys. Lett. 275 (1997) 46.

[28] S. B. Boys and F. Bernardi Molecular Physics 19 (1970) 533.

[29] H. J. Monkhorst and J. D. Pack Phys. Rev. B. 13 (1976) 5188.

[30] D. M. Ceperley and B. J. Alder Phys. Rev. Lett. 45 (1980) 566.

[31] A. Maeland and T. B. Flanagan Canadian journal of Physics 42 (1964) 2364.

[32] W. Andreoni and A. Curioni Applied Physics a 66 (1998) 299.

[33] C. M. Vargas, P. Gianozzi, A. Selloni, and G. Scoles J. Phys. Chem 105 (2001) 9509.

[34] C. Hofner and J. W. Rabalais Surf. Sci. 400 (1998) 189.

[35] M. Guillope and B. Legrand Surface Science 215 (1989) 577.

[36] K. M. Beardmore, J. D. Kress, A. R. Bishop, and N. Grøbech-Jensen Synthetic Metals 84 (1997) 317.

[37] H. Sellers, A. Ulman, and Y. Shnidman Journal of the American Chemical Society 115 (1993) 9389.

[38] T. Hayashi, Y. Morikawa, and H. Nozoye J. Chem. Phys. 114 (2001) 7615.

[39] D. Fischer, A. Curioni, and W. Andreoni Langmuir 19 (2003) 3567.

[40] C. Majumder, T. M. Briere, H. Mizuseki, and Y. Kawazoe J. Chem. Phys. 117 (2002) 2819

Figure Captions

Figure 1. Total energy of the thiol molecule and bulk gold as a function of orbital confinement. Energy shift is the orbital excitation energy due to orbital confinement, as the energy shift tends to zero the confinement tends to zero.

Figure 2. Energy for bulk gold unit cell as a function of number of k-points. Total energy is given relative to energy for a single k-point.

Figure 3. Illustration of the facets presented on an idealised 236 atom Au cluster, the darker atoms in each case indicate the facet of interest. Below, the corresponding surfaces used for simulation purposes are shown, with the calculated adsorption sites indicated.

Figure 4. Optimised adsorption geometries for SCH_3 on Au(111) surface. Each configuration is shown as viewed from the side (left) and from the top (right). Initial starting points are those illustrated in the lower, left item of Figure 3.

Figure 5. Total energy of Au(111)-SCH_3 system as a function of distance from the surface at the various adsorption sites.

Figure 6. Geometry optimised configurations of SCH_3 on Au(110) missing row reconstructed surface. Each configuration is shown as viewed from the side (left) and from the top (right). Initial starting points are those illustrated in the lower, centre item of Figure 3. Arrows on the extreme right of the figure indicate direction of the side-views.

Figure 7. Geometry optimised configurations of SCH_3 on Au(100) surface. Each configuration is shown as viewed from the side (left) and from the top (right). Initial starting points are those illustrated in the lower, right item of Figure 3.

Table 1. Relaxation of five layer slabs with (111), (110) and (100) surface symmetries.

	(111)			(110)			(100)		
layer	***d (Å)***	***Δd (Å)***	***Δd(%)***	***d (Å)***	***Δd (Å)***	***Δd(%)***	***d (Å)***	***Δd (Å)***	***Δd(%)***
d_{45}	2.406	-0.01	-0.48	1.184	-0.296	-20.00	2.051	-0.025	-1.22
d_{34}	2.363	-0.05	-2.25	1.653	-0.123	-8.31	2.087	-0.015	-0.73
d_{23}	2.361	-0.06	-2.35	1.290	-0.313	-21.17	2.082	-0.010	-0.50
d_{12}	2.383	-0.03	-1.43	1.436	-0.357	-24.16	2.059	-0.029	-1.38

Table 2. Adsorption energies for SCH_3 on Au(111) obtained by geometry optimisation with the starting configurations at the sites indicated on Figure 3.

Initial site	***E_{ads} (kCal.mol-1) (111) (Final Site)***	***E_{ads} (kCal.mol-1) (110)***	***E_{ads} (kCal.mol-1) (100)***
a	-31.12 (fcc)		
b	-39.26 (fcc)		
c	-38.91 (Bridge)		
d	-34.52 (hcp)		
e			
f			
g			
h			

Table 3. Comparison of results presented within the surveyed literature for calculated adsorption of SCH_3 on the Au(111) surface.

Ref	***Calculation Type and XC functional***		***Relativistic***	***Slab or cluster?***	***Preferred site***	***E_{ads} (kCal mol-1)***	***$D_{Au(111)-S}$ (Å)***	***Tilt (deg)***
This work	LCAO	PBE	Yes	5 layer slab	bridge	39.26	2.07	42
Yourdshahan *et al* [20]	PW	PW91, RPBE	No	6+7 layer slab	"between hollow and bridge"	39.96	2.03	43.2
Andreoni *et al* [19]	PW	BLYP, PBE	Yes	4 layer slab	fcc	55	n/a	n/a
Beardmore *et al* [18,36]	LCAO	LYP	Yes	17 atom cluster	hcp	n/a	n/a	0
Sellers *et al* [37]	HF		Yes	cluster	hcp	n/a	1.905	0
Hayashi *et al* [38]	PW	PBE	Yes	4 layer slab	bridge	12.47	n/a	52.7
Vargas *et al* [33]	PW	PW91	Yes	4 layer slab	bridge	18.6	2.09	58
Molina and Hammer [21]	PW	PW91, RPBE	n/a	4 & 5 layer slab	bridge	38.5, 26.1	n/a	63
Majumder *et al* [40]	PW	PW91	n/a	cluster	fcc	53.8	n/a	n/a

Table 4. Adsorption energies for SCH_3 on Au(110) at the sites indicated on Figure 3.

site	E_{ads} *(kCal.mol^{-1})*	*Tilt (deg)*	$D_{Au\text{-}S}$ *(Å)*
a	-51.10	33.0	2.46, 2.46, 3.26
b	-51.04	17.4	2.46, 2.47, 3.16
c	-46.04	0.7	2.46, 2.46, 2.81
d	-41.04	38.5	2.54, 3.13, 3.59
e	-50.94	15.9	2.47, 2.45, 4.31
f	-47.75	15.91	2.45, 2.46, 2.74
g	-47.68	14.47	2.45, 2.46, 2.71
h	-36.38	9.3	2.56, 2.81, 2.62

Table 5. Adsorption energies for SCH_3 on Au(100) at the sites indicated on Figure 3.

Site	E_{ads} *(kCal.mol^{-1})*	*Tilt (deg)*	$D_{Au\text{-}S}$ *(Å)*
a	-43.77	42.4	2.48
b	-48.38	49.0	2.47, 2.46
c	-43.48	3.1	2.70, 2.62, 2.72, 2.56

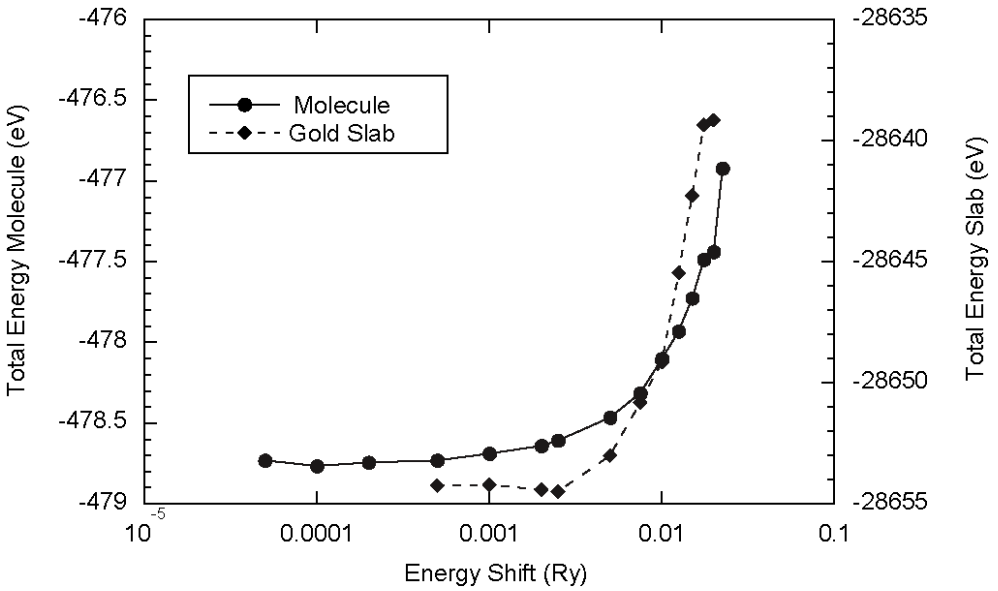
-476
-476.5
-477
-477.5
-478
-478.5
-479
-28635
-28640
-28645
-28650
-28655
Molecule
Gold Slab
Total Energy Molecule (eV)
Total Energy Slab (eV)
10 -5
0.0001
0.001
0.01
0.1
Energy Shift (Ry)

Figure 1.

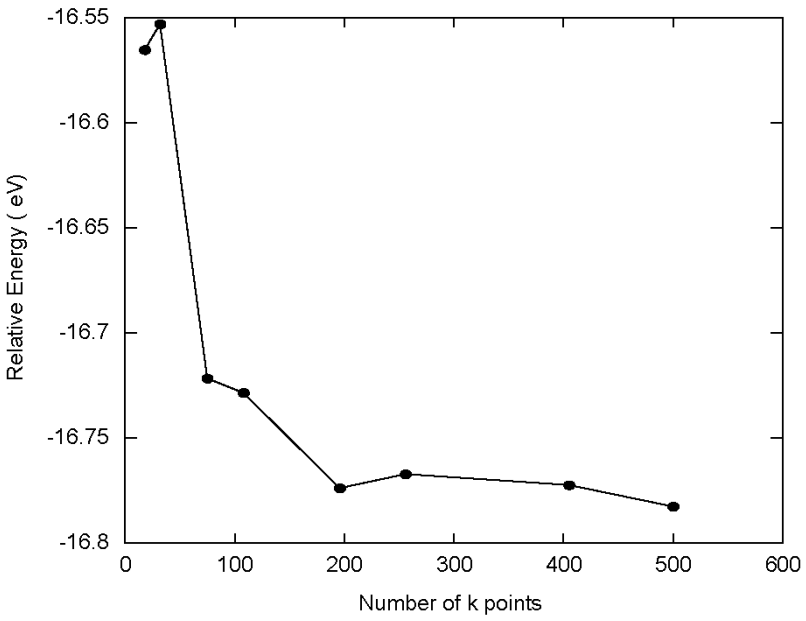
-16.55
-16.6
-16.65
-16.7
-16.75
-16.8
Relative Energy (eV)
0
100
200
300
400
500
600
Number of k points

Figure 2.

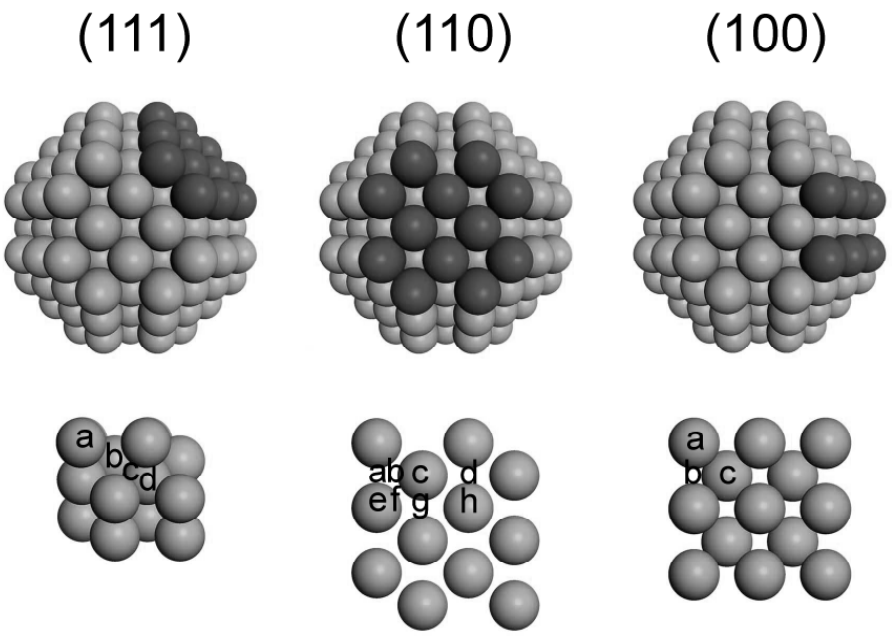

Figure 3.

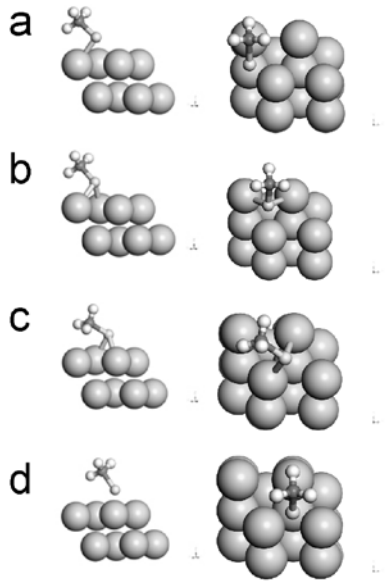

Figure 4.

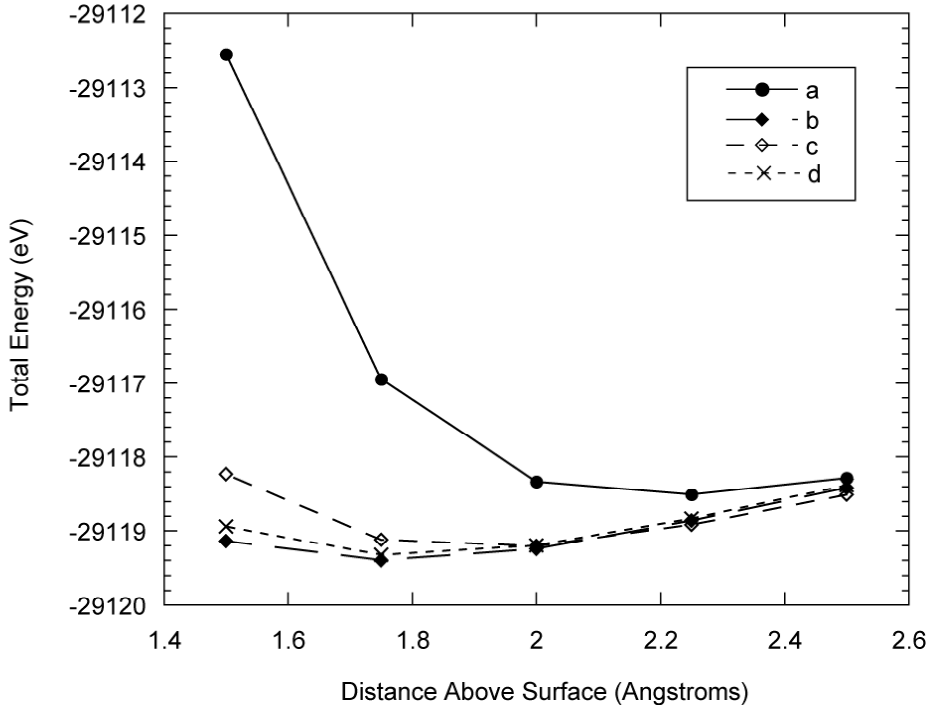
-29112
-29113
-29114
-29115
-29116
-29117
-29118
-29119
-29120
Total Energy (eV)
1.4
1.6
1.8
2
2.2
2.4
2.6
Distance Above Surface (Angstroms)
a
b
c
d

Figure 5.

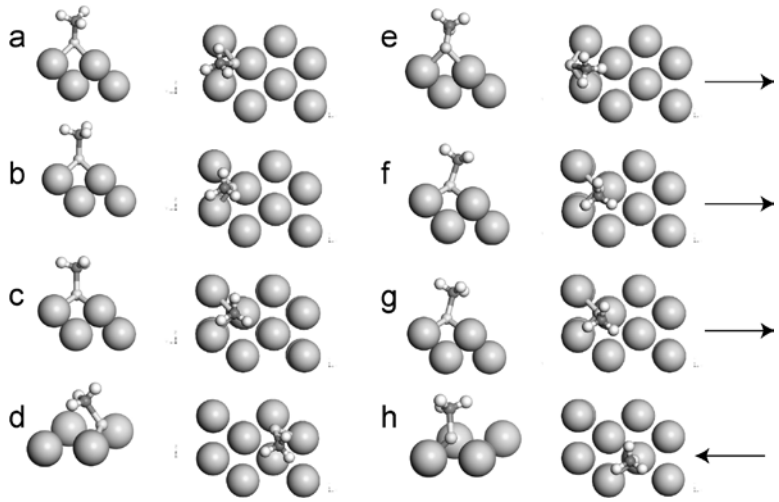

Figure 6.

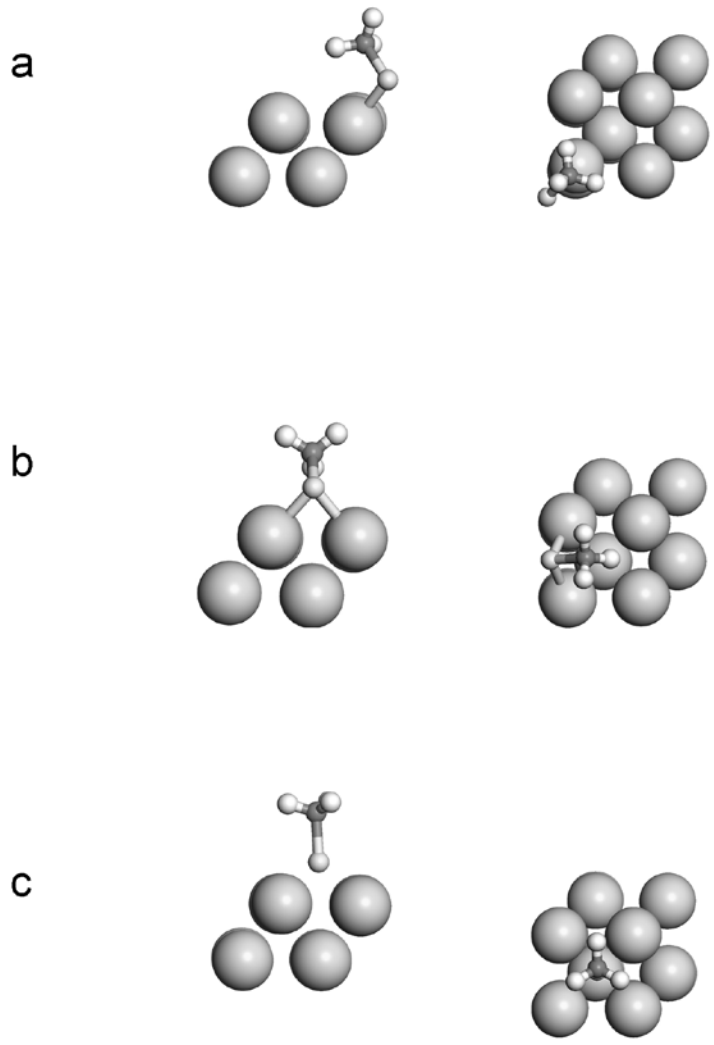

Figure 7.